Anal. Chem. **2008,** *80,* 5094–5102

Activity-Based Assay of Matrix Metalloproteinase on Nonbiofouling Surfaces Using Time-of-Flight Secondary Ion Mass Spectrometry

Young-Pil Kim,[†] Bong Soo Lee,[‡] Eunkyung Kim,[†] Insung S. Choi,[‡] Dae Won Moon,[§] Tae Geol Lee,[§] and Hak-Sung Kim*,[†]

Department of Biological Sciences, KAIST, Daejeon 305-701, Korea, Department of Chemistry and School of Molecular Science (BK21), Center for Molecular Design and Synthesis, KAIST, Daejeon 305-701, Korea, and Nanobio Fusion Research Center, Korea Research Institute of Standards and Science (KRISS), Daejeon 305-600, Korea

A label-free, activity-based assay of matrix metalloproteinase (MMP) and its inhibition was demonstrated on peptide-conjugated gold nanoparticles (AuNPs) with nonbiofouling poly(oligo(ethylene glycol) methacrylate) (*p*OEGMA) films using time-of-flight secondary ion mass spectrometry (TOF-SIMS). Following surface-initiated atom-transfer radical polymerization of OEGMA on a Si/SiO_2 substrate, the MMP activity was determined by analyzing the cleaved peptide fragments using TOF-SIMS on the peptide-conjugated AuNPs. The use of nonbiofouling *p*OEGMA films in conjunction with AuNPs synergistically enhanced the sensitivity of assays for MMP activity and its inhibition in human serum. The detection sensitivity of MMP-7 in serum was as low as 20 ng mL^{-1} (1 pmol mL^{-1}), and the half-maximal inhibitory concentration (IC_{50}) of minocycline, which is a MMP-7 inhibitor, was estimated to be 450 nM. It is anticipated that the developed system will be broadly useful for conducting activity-based assays of serum proteases, as well as for screening of their inhibitors, with high sensitivity in a high-throughput manner.

Matrix metalloproteinases (MMPs) are zinc-dependent endopeptidases that mediate the dynamic regulation of many functions in cells through the degradation of the extracellular matrix, and their aberrant expression is known to be linked with various diseases.[1–3] In human, the MMP family consists of more than 21 members that share significant sequence homology. They have different molecular masses and also display diverse substrate cleavage sites.[4] Because MMPs have been reported to be upregulated in almost all human cancerous cells and in malignant tissues, the level of MMPs in human serum is of great significance as a promising prognostic marker.[5,6] In addition, MMP inhibitors have also been recognized as drug candidates for anticancer therapeutics.[7–9] With the increasing demand for diagnostics and therapeutics against MMP-related diseases and other disorders, much effort has been made to develop effective methods to assay MMPs and their inhibitors. To date, most reported MMP assay platforms have relied on affinity-based methods such as immunoassay.[10,11] As a more specific approach, activity-based assays employing fluorophore-tagged substrates[12–17] have also been developed for increased utility in diagnostics and drug discovery applications. However, the labeling of substrates with various fluorophores is often a complicated step and can also significantly alter enzyme activity. Furthermore, fluorescent labels tend to increase the amount of background noise especially in serum samples, thus diminishing the reliability of analyses due to false-positive signals.

As a label-free approach, mass spectrometry (MS) has attracted much attention for assays of enzyme activity with high sensitivity and specificity because it relies on the intrinsic mass signal of a target molecule.[18–20] A recent development in this area is self-

* To whom correspondence should be addressed. Phone: +82-42-869-2616. Fax: +82-42-869-2610. E-mail: hskim76@kaist.ac.kr.

[†] Department of Biological Sciences, KAIST.

[‡] Department of Chemistry and School of Molecular Science, Center for Molecular Design and Synthesis, KAIST.

[§] Korea Research Institute of Standards and Science.

(1) Egeblad, M.; Werb, Z. *Nat. Rev. Cancer* **2002**, *2*, 161–174.
(2) Johnson, L. L.; Dyer, R.; Hupe, D. J. *Curr. Opin. Chem. Biol.* **1998**, *2*, 466–471.
(3) Overall, C. M.; Kleifeld, O. *Nat. Rev. Cancer* **2006**, *6*, 227–239.
(4) McCawley, L. J.; Matrisian, L. M. *Curr. Opin. Cell Biol.* **2001**, *13*, 534–540.
(5) Lein, M.; Nowak, L.; Jung, K.; Koenig, F.; Lichtinghagen, R.; Schnorr, D.; Loening, S. A. *Clin. Biochem.* **1997**, *30*, 491–496.
(6) Nikkola, J.; Vihinen, P.; Vuoristo, M. S.; Kellokumpu-Lehtinen, P.; Kahari, V. M.; Pyrhonen, S. *Clin. Cancer Res.* **2005**, *11*, 5158–5166.
(7) Coussens, L. M.; Fingleton, B.; Matrisian, L. M. *Science* **2002**, *295*, 2387–2392.
(8) Denis, L. J.; Verweij, J. *Invest. New Drugs* **1997**, *15*, 175–185.
(9) Hidalgo, M.; Eckhardt, S. G. *J. Natl. Cancer Inst.* **2001**, *93*, 178–193.
(10) Laack, E.; Kohler, A.; Kugler, C.; Dierlamm, T.; Knuffmann, C.; Vohwinkel, G.; Niestroy, A.; Dahlmann, N.; Peters, A.; Berger, J.; Fiedler, W.; Hossfeld, D. K. *Ann. Oncol.* **2002**, *13*, 1550–1557.
(11) Ohuchi, E.; Azumano, I.; Yoshida, S.; Iwata, K.; Okada, Y. *Clin. Chim. Acta* **1996**, *244*, 181–198.
(12) Srinivasan, R.; Huang, X.; Ng, S. L.; Yao, S. Q. *Chembiochem* **2006**, *7*, 32–36.
(13) Sun, H.; Chattopadhaya, S.; Wang, J.; Yao, S. Q. *Anal. Bioanal. Chem.* **2006**, *386*, 416–426.
(14) Harris, J. L.; Backes, B. J.; Leonetti, F.; Mahrus, S.; Ellman, J. A.; Craik, C. S. *Proc. Natl. Acad. Sci. U. S. A.* **2000**, *97*, 7754–7759.
(15) Levine, L. M.; Michener, M. L.; Toth, M. V.; Holwerda, B. C. *Anal. Biochem.* **1997**, *247*, 83–88.
(16) Salisbury, C. M.; Maly, D. J.; Ellman, J. A. *J. Am. Chem. Soc.* **2002**, *124*, 14868–14870.
(17) Kim, Y.-P.; Oh, Y.-H.; Oh, E.; Kim, H.-S. *Biochip J.* **2007**, *1*, 228–233.
(18) Aebersold, R.; Mann, M. *Nature* **2003**, *422*, 198–207.
(19) Greis, K. D. *Mass Spectrom. Rev.* **2007**, *26*, 324–339.
(20) Lee, C.-S.; Song, H.-M.; Kang, K.-K.; Choi, C.-H.; Rhee, H.-K.; Kim, B.-G. *Biochip J.* **2007**, *1*, 43–48.

10.1021/ac800299d CCC: $40.75
Published on Web 05/28/2008

assembled matrix-assisted laser desorption/ionization MS, which employs self-assembled monolayers (SAMs) of oligo(ethylene glycol) (OEG)-terminated alkanethiols to block the adsorption of interfering biomolecules.[21–23] Indeed, this method was reported to be very effective for the high-throughput screening of small drugs and target proteins. Another technique, time-of-flight secondary ion mass spectrometry (TOF-SIMS), has also been of great interest due to its potential for the chemical imaging of organic biosurfaces. In addition to its surface sensitivity (information depth is typically 10−15 Å), TOF-SIMS is a typically matrix-free analytical system. In the case of MALDI-MS, reproducibility of the signal might be affected by the use of matrix. On the other hand, matrix-free SIMS usually gives the reproducible results with high sensitivity and chemical specificity.[24,25] Nonetheless, widespread application of the technique has been hindered by its limited mass range and the low secondary ion (SI) yield of biomolecules. In an effort to increase the SI yield and thereby enhance the detection sensitivity in enzyme activity assays, the use of substrate-conjugated gold nanoparticles (AuNPs) has been explored.[26,27] However, blockage of nonspecific protein bindings on the nanoparticle-attached surfaces still remains crucial for optimal performance. Various methods can be used to achieve this, including the use of $(EG)_n$-terminated alkanethiols,[22] poly(ethylene glycol),[28] and various peptide/protein species.[29] However, all of these approaches display only limited efficacy whenever a complex protein mixture, such as human serum, is analyzed, due to the relatively low surface density of exogenous molecules that results from their limited volume capacity and steric hindrance effects.[30,31]

Here we describe an activity-based assay of MMP and its inhibition on peptide-conjugated AuNPs with nonbiofouling poly(oligo(ethylene glycol) methacrylate) (*p*OEGMA) films using TOF-SIMS. Following surface-initiated atom-transfer radical polymerization (SI-ATRP) of oligo(ethylene glycol) methacrylate (OEGMA) on a Si/SiO_2 substrate, monolayers of AuNPs were formed. SI-ATRP has proven to be effective for preventing nonspecific protein adsorptions when compared to other methods since it gives rise to a high surface density of polymers and a dense brush layer of pendant oligo(ethylene glycol) moieties.[32–34] For the protease assays conducted in this work, cysteine-terminated peptides were adsorbed onto the AuNPs, and the cleaved peptide fragments were analyzed using TOF-SIMS.

MATERIALS AND METHODS

Materials. Matrix metalloproteinase-7 (MMP-7) and matrix metalloproteinase-2 (MMP-2) were purchased from Calbiochem and Sigma, respectively. Cysteine-terminated peptide substrates (Ac-RPLALWRSC and Ac-RPLALWRSCGGGC) were synthesized from Peptron Inc. Minocycline (MMP inhibitor) was obtained from Sigma. 3-Aminopropyltriethoxysilane (APTES, 99%) and 11-amino-1-undecanethiol (AUT, 99%) were purchased from Aldrich and Dojindo, respectively. A chambered silicon coverslip (3 mm × 1 mm, sterile) was from Sigma-Aldrich. Other chemical reagents were used as received: OEGMA (M_n: ~360, Aldrich), copper(I) bromide (99.999%, Aldrich), 2,2-dipyridyl (bpy, 99+%, Aldrich), *N,N*-disuccinimidyl carbonate (DSC, Aldrich), 4-(dimethylamino)pyridine (DMAP, Fluka), 2-(2-aminoethoxy)ethanol (EG_2-NH_2, 98%, Aldrich), ethylenediamine (99+%, Aldrich), and $BrC(CH_3)_2COO(CH_2)_3Si(OCH_3)_3$ (TBMP, Gelest), absolute ethanol (99.9+%, Merck), absolute methanol (99.9+%, Merck), anhydrous *N,N*′-dimethylformamide (DMF, 99.8+%, Aldrich), toluene (J. T. Baker), hydrogen tetrachloroaurate(III) trihydrate (99.9% $HAuCl_4 \cdot 3H_2O$, Sigma-Aldrich), sodium citrate dihydrate (99.9%, 2-hydroxy-1,2,3-propanetricarboxylic acid trisodium salt, $C_6H_5Na_3O_7 \cdot 2H_2O$, Sigma), and sodium borohydride (99%, Sigma-Aldrich).

Construction and Activation of the *p*OEGMA Films. (i) Preparation of SAMs of ATRP Initiators. The *p*OEGMA films were prepared by atom-transfer radical polymerization of surface-immobilized initiators according to methods described elsewhere.[33,34] SAMs of ATRP initiators were formed on Si/SiO_2 (Scheme 1). The Si/SiO_2 substrate (Si or glass) was cleaned for 2 min in piranha solution (3:7 by volume of 30% H_2O_2 and H_2SO_4. Safety note: Piranha solutions can react violently with organic materials.), rinsed with H_2O and ethanol, and then dried under a stream of argon. The substrates were subsequently treated with O_2-plasma and immersed in a solution of TBMP (5 mM in toluene) at room temperature overnight. Following the formation of the SAMs, the substrates were thoroughly rinsed with toluene and ethanol several times and then dried in a stream of argon.

(ii) Surface-Initiated ATRP (SI-ATRP) of OEGMA. We used 1 M OEGMA to obtain *p*OEGMA films with various thicknesses on Si/SiO_2 substrates. To a Schlenk tube containing deionized water (degassed, 1.34 mL) and methanol (degassed, 5.39 mL) were added Cu(I)Br (143 mg, 1 mmol), bpy (312 mg, 2 mmol), and OEGMA (3.26 mL, 10 mmol). The resulting dark-red solution was bubbled with Ar gas for 10 min. SI-ATRP was initiated by transferring the mixture to a degassed Schlenk tube that contained a Si/SiO_2 substrate presenting ATRP initiators, and then the mixture was soaked for a specified time (2−1200 min) under argon at room temperature. The polymerization was terminated by exposing the reaction to air and pouring water into the Schlenk tube. The termination step caused the reaction solution to turn blue, indicating the oxidation of Cu(I) to Cu(II). All the *p*OEGMA-coated substrates were thoroughly washed with deionized water and methanol in order to remove any physisorbed polymers and then dried in a stream of argon.

(iii) Activation of *p*OEGMA Films with DSC and Subsequent Coupling of Ethylenediamine. To activate the terminal hydroxyl groups of the side chains in the *p*OEGMA films, we

(21) Min, D. H.; Tang, W. J.; Mrksich, M. *Nat. Biotechnol.* **2004**, *22*, 717–723.
(22) Su, J.; Mrksich, M. *Angew. Chem., Int. Ed.* **2002**, *41*, 4715–4718.
(23) Su, J.; Rajapaksha, T. W.; Peter, M. E.; Mrksich, M. *Anal. Chem.* **2006**, *78*, 4945–4951.
(24) Belu, A. M.; Graham, D. J.; Castner, D. G. *Biomaterials* **2003**, *24*, 3635–3653.
(25) Vickerman, J. C.; Briggs, D. *ToF-SIMS: Surface analysis by mass spectrometry*; SurfaceSpectra: Manchester, UK, 2001.
(26) Kim, Y. P.; Oh, E.; Oh, Y. H.; Moon, D. W.; Lee, T. G.; Kim, H. S. *Angew. Chem., Int. Ed.* **2007**, *46*, 6816–6819.
(27) Kim, Y. P.; Oh, E.; Hong, M. Y.; Lee, D.; Han, M. K.; Shon, H. K.; Moon, D. W.; Kim, H. S.; Lee, T. G. *Anal. Chem.* **2006**, *78*, 1913–1920.
(28) Yang, Z.; Galloway, J. A.; Yu, H. *Langmuir* **1999**, *15*, 8405–8411.
(29) Moreno-Bondi, M. C.; Taitt, C. R.; Shriver-Lake, L. C.; Ligler, F. S. *Biosens. Bioelectron.* **2006**, *21*, 1880–1886.
(30) Knoll, D.; Hermans, J. *J. Biol. Chem.* **1983**, *258*, 5710–5715.
(31) Ejaz, M.; Yamamoto, S.; Ohno, K.; Tsujii, Y.; Fukuda, T. *Macromolecules* **1998**, *31*, 5934–5936.
(32) Ma, H.; Hyun, J.; Stiller, P.; Chilkoti, A. *Adv. Mater.* **2004**, *16*, 338–341.
(33) Lee, B. S.; Chi, Y. S.; Lee, K. B.; Kim, Y. G.; Choi, I. S. *Biomacromolecules* **2007**, *8*, 3922–3929.
(34) Lee, B. S.; Lee, J. K.; Kim, W. J.; Jung, Y. H.; Sim, S. J.; Lee, J.; Choi, I. S. *Biomacromolecules* **2007**, *8*, 744–749.

Scheme 1. Procedure for Synthesizing the *p*OEGMA Films, and the General Principle Behind the Analysis of Matrix Metalloproteinase Activity Using Secondary Ion Mass Spectrometry on Surfaces Containing Peptide-Conjugated Gold Nanoparticles[a]

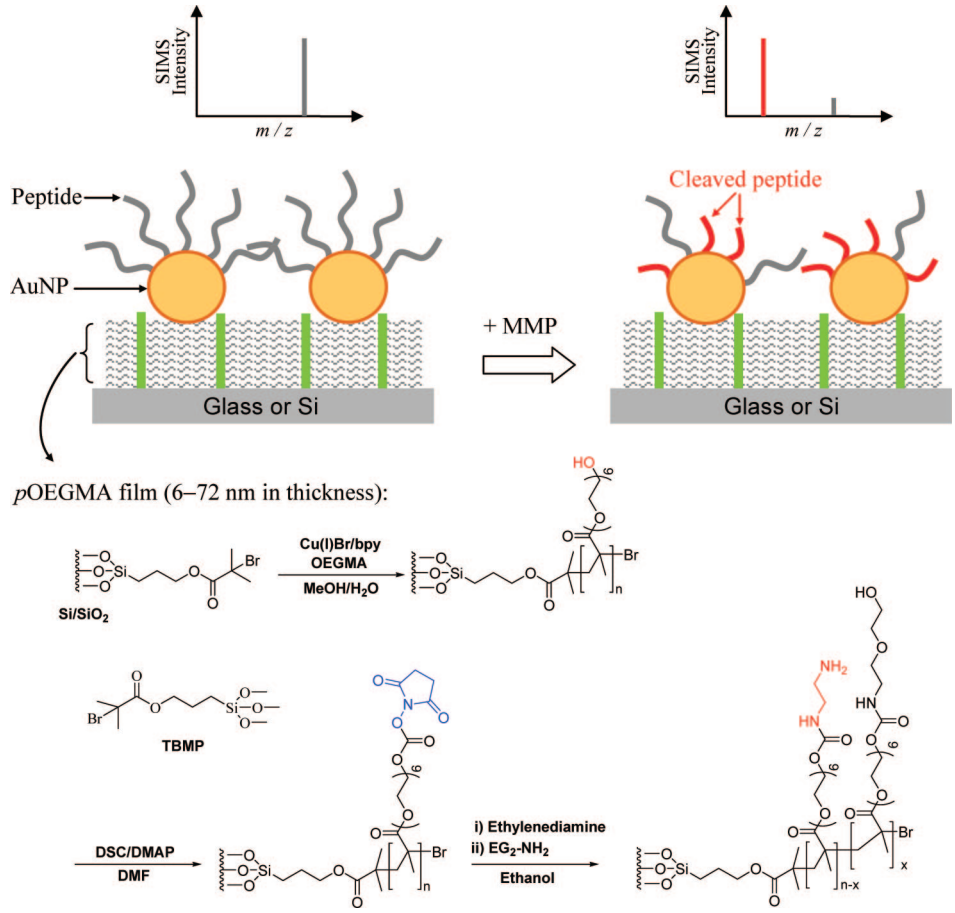

[a] AuNPs were electrostatically attached onto poly(oligo(ethylene glycol) methacrylate) (*p*OEGMA) films chemically modified with an amine functional group.

immersed the films in dry DMF solution containing 0.1 M DSC and 0.1 M DMAP for 14 h at room temperature under an Ar atmosphere.[33] The resulting substrates were rinsed with DMF and CH_2Cl_2 and dried in a stream of Ar. The DSC-activated films were then soaked in ethylenediamine (10% v/v in deionized water) for 2 h at room temperature to generate NH_2-functionalized *p*OEGMA films. Following this reaction step, the substrates were washed with deionized water and dried in a stream of Ar. Any remaining NHS carbonate ester groups were subsequently deactivated by immersing the substrates in a 10% ethanol solution of EG_2-NH_2 for 2 h at room temperature. After treating with blocking agent, the substrates were rinsed with ethanol and then dried in a stream of Ar.

Ellipsometric Analysis. The thicknesses of the monolayer and polymer films were measured with a Gaertner L116s ellipsometer (Gaertner Scientific Corp., Chicago, IL) equipped with a He−Ne Laser (632.8 nm) at a 70° angle of incidence. A refractive index of 1.46 was used for all films.

Synthesis of AuNPs. AuNPs were synthesized by reduction and stabilization with citrate as described previously.[21] The clustering of AuNPs was checked by UV−visible spectroscopy (UV-2550, Shimadzu). The average size of the AuNPs on the Si/SiO_2 surface was estimated to be 10.7 ± 2.7 nm by using a field-emission scanning electron microscope (Sirion, FEI).

Protease Assay. A multiwell-type chambered silicon coverslip (50 wells, 3 mm in diameter and 1 mm in height) was overlaid on the NH_2-functionalized *p*OEGMA films with the reaction area in each well exposed. A solution of 10 nM AuNPs (100 μL) in deionized water was added to the wells and incubated for 30 min at room temperature to allow electrostatic adsorption of the AuNPs. The wells were washed vigorously with deionized water three times by pipetting and then dried. Two different peptides (Ac-RPLALWRSC and Ac-RPLALWRSGGGC) were dissolved in 25 mM HEPES buffer (pH 7.4) to give a final concentration of 50 μg mL^{-1}, and each was immobilized onto the monolayer of AuNPs in separate wells. The resulting surface was sequentially washed with deionized water and dried under a stream of N_2. The protease reaction was initiated by addition of a reaction mixture (10 μL) containing MMP to the wells and incubated at 37 °C for 60 min. The reaction mixture contained MMP-7 or MMP-2 (ranging from 2 ng mL^{-1} to 20 μg mL^{-1}) either in human serum or in 50 mM HEPES buffer (pH 7.4, containing 150 mM NaCl, 1 mM $MgCl_2$, and 1 mM $CaCl_2$). In the case of serum mixture, a 10 μL of 1/4-diluted solution with HEPES buffer was incubated on the surface. The resulting surface was washed vigorously with deionized water several times, dried, and subjected to TOF-SIMS analysis. Reaction with MMP-7 led to the loss of an N-terminal peptide segment from the immobilized peptide substrate, and a mass spectrum with a

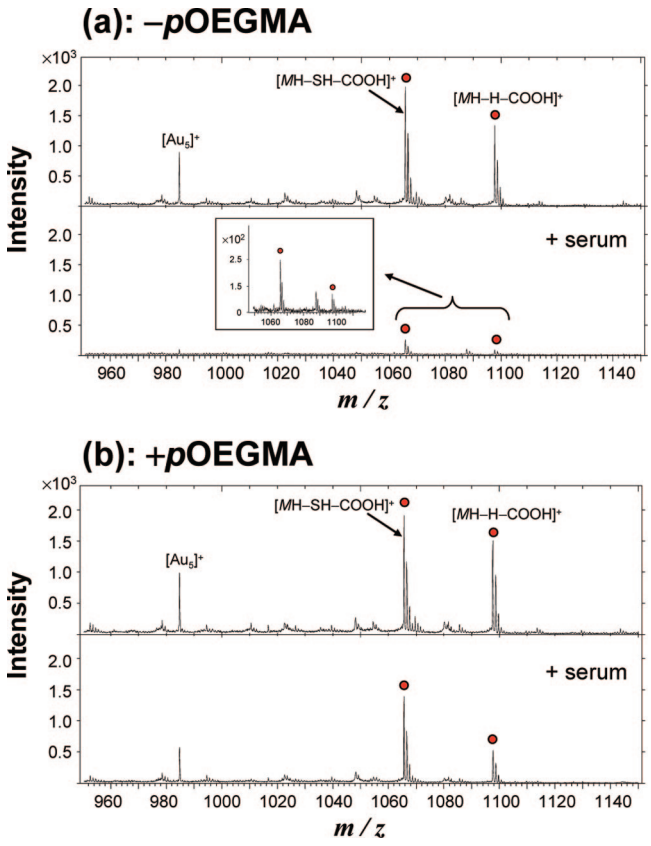

Figure 1. Changes in SIMS spectra from the peptide (Ac-RPLAL-WRSC, $M_r = 1142.60$) after serum adsorption (a) in the absence and (b) in the presence of *p*OEGMA films. The characteristic peaks of the peptide are marked in a red circle. The inset in (a) is a magnified view of low peak intensity. Human normal serum was adsorbed for 60 min onto the respective surfaces followed by washing with buffer and distilled water. The thickness of the *p*OEGMA film was 27 nm.

new peak was observed. This peak corresponds to the peptide remaining on AuNPs after cleavage by MMP-7. For the inhibition assays, a stock solution (1 mM) of minocycline was diluted to different concentrations in 50 mM HEPES (pH 7.4) as appropriate and added to the reaction mixture.

As a control, a bare gold substrate was prepared by evaporating a 2-nm-thick film of Ti and a 40-nm-thick film of Au onto a Si wafer. The resulting gold substrates were cleaned using piranha solution. Following the chemisorption of cysteine-terminated peptides to the bare gold substrate, protease activity was assayed as described above. A Si/SiO_2/APTES surface was prepared by immersing the Si/SiO_2 substrate in a solution of APTES (2 mM in absolute ethanol) for 12 h. Following rinses with deionized water and drying under a stream of N_2, the resulting surfaces were used for the protease assays.

Surface Plasmon Resonance (SPR) Spectroscopy. SPR analysis was performed using a BIAcore-X instrument and gold sensor chips (BIAcore). The chip surface was first cleaned with 0.1 N NaOH containing 0.1% Triton-X for 5 min. For the synthesis of *p*OEGMA on gold, $[BrC(CH_3)_2COO(CH_2)_{11}S]_2$ was prepared as described elsewhere.[34] The SAMs of $[BrC(CH_3)_2COO(CH_2)_{11}S]_2$ were prepared by immersing the gold substrate in a 1 mM ethanol solution of $[BrC(CH_3)_2COO(CH_2)_{11}S]_2$ for 12 h at room temperature. To obtain an NH_2-functionalized *p*OEGMA film on the SPR gold chip, SAMs of disulfide initiators, SI-ATRP

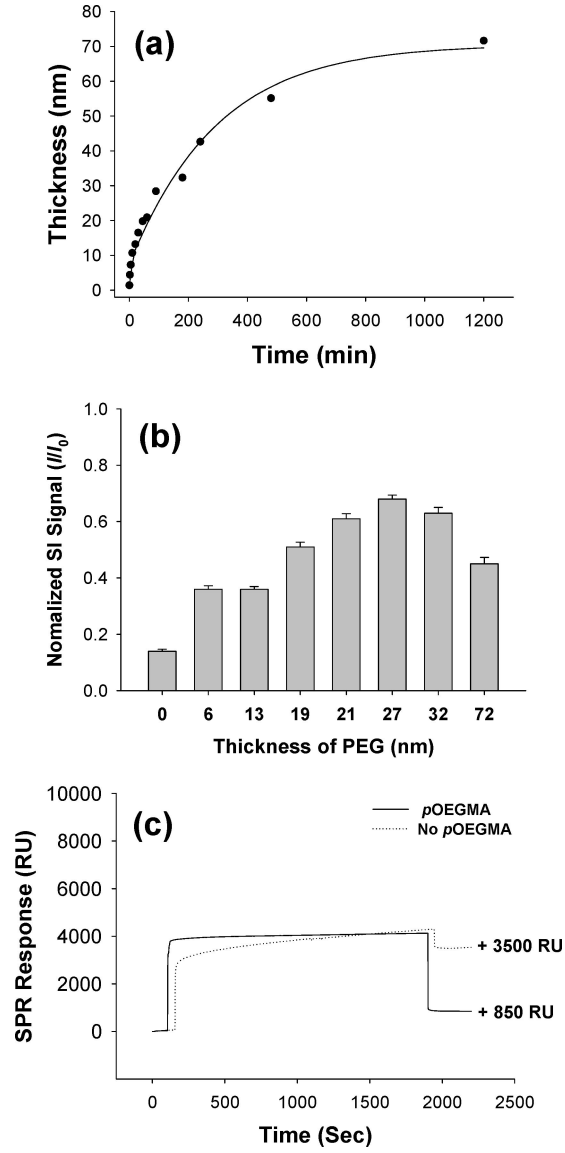

Figure 2. (a) Graph of the ellipsometric thickness of *p*OEGMA films on Si/SiO_2 versus polymerization time. (b) Effect of *p*OEGMA film thickness on the adsorption of serum proteins in SIMS analyses. The peak intensity (I) of the peptide at $[MH\text{-SH-COOH}]^+$ after serum treatment was normalized to the corresponding peak intensity (I_0) before serum treatment on the respective surfaces. The error bars indicates the standard deviation from three different areas on the same sample surface. (c) Binding isotherm of human serum from SPR spectroscopy in the presence (solid line) and absence (dotted line) of *p*OEGMA films.

of OEGMA, DSC activation, amination by ethylenediamine, and blocking of EG_2-NH_2 were all performed using procedures similar to those described above for the Si/SiO_2 substrates. As a control surface, an AUT-modified gold surface was prepared by immersing the SPR gold chip in a 2 mM ethanolic solution of AUT for 2 h, followed by thorough rinsing with absolute ethanol and deionized water. Both the *p*OEGMA- and AUT-modified gold surfaces were then subjected to further modifications, namely, the attachment of AuNPs and the conjugation of peptide. The final, modified gold sensor chips were independently docked into the Biacore instrument and prerinsed with running buffer (50 mM HPEPS buffer, pH 7.4). To comparatively evaluate the SPR signals arising from the

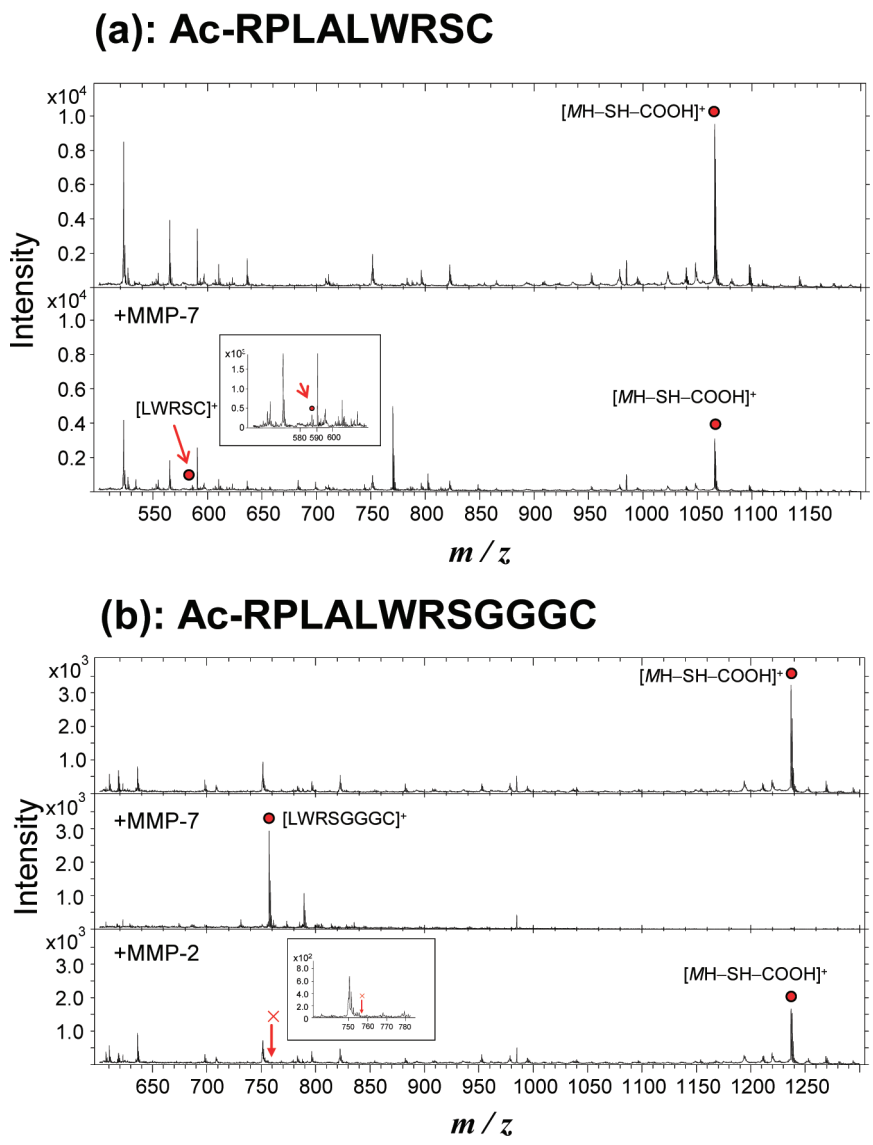

Figure 3. SIMS spectra generated by the action of MMP-7 for peptide substrates with different lengths: (a) Ac-RPLALWRSC (M_r = 1142.60) and (b) Ac-RPLALWRSGGGC (M_r = 1313.67). The peaks of *m/z* 1066 and 1237 indicate the quasi-molecular ions ([*M*H-SH-COOH]$^+$) from the respective peptides. The peaks of *m/z* 586 ([LWRSC]$^+$) and 757 ([LWRSGGGC]$^+$) correspond to the proteolytic cleavage masses of Ac-RPLALWRSC and Ac-RPLALWRSGGGC, respectively. The inset is a magnified view of low peak intensity. MMP-7 (100 ng mL^{-1} in HEPES, pH 7.4) was added and incubated for 60 min at 37 °C on the respective surfaces. AuNPs were deposited onto the *p*OEGMA films (27 nm in thickness) followed by conjugation with the peptide substrate.

nonspecific binding of proteins, a solution containing 1/4-diluted serum was flowed over the sensor surfaces for 30 min at a flow rate of 2 μL min^{-1} at 25 °C.

TOF-SIMS Analysis. Ion spectra measurements by TOF-SIMS were carried out with a TOF-SIMS V instrument (ION-TOF GmbH) using a 25-keV Bi_1^+ primary ion beam source. The ion currents were measured to be 0.5 pA (Bi_1^+) at 5 kHz using a Faraday cup located at the grounded sample holder. A pulse with of 0.7 ns from the bunching system resulted in mass resolution exceeding $M/\Delta M = 10^4$ (full width at half-maximum) at m/z < 500 in both the positive and negative modes. The analysis area (500 × 500 μm^2) was randomly rastered by the primary ions, and the primary ion dose was maintained below 10^{12} ions cm^{-2} to ensure static SIMS conditions. Positive ion spectra were internally calibrated by using the H^+, H_2^+, CH_3^+, $C_2H_3^+$, and $C_3H_4^+$ signals.

Calculation of Peptide Cleavage Efficiency and IC_{50} Values. The cleavage efficiency of the protease reaction was calculated by using the following formula:

$$\text{cleavage efficiency (\%)} = \frac{I_C}{I_P + I_C} \times 100 \qquad (1)$$

where I_p is the peak intensity of [*M*H-SH-COOH]$^+$ ions arising from the uncleaved original peptide (molecular weight = M) and I_c is the peak intensity of [M_cH-SH-COOH]$^+$ ions arising from cleaved peptide (molecular weight = M_c). The I_P and I_c values were calculated after normalization against the background intensity. For the inhibition assays, the cleavage efficiencies were plotted as a function of the inhibitor concentration and then fitted to a four-parameter logistic function (dose−response model for ligand binding) by using the nonlinear regression procedure

Table 1. Cleavage Efficiency of MMP for Peptide Substrates at Different Surfaces

peptide substrate	protease[b]	surface[c]	cleavage efficiency (%)[d]
Ac-RPLALWRSC[a]	MMP-7	SiO_2/pOEGMA/AuNP	9.6 ± 3.4
Ac-RPLALWRSGGGC[a]	MMP-7	SiO_2/pOEGMA/AuNP	93.6 ± 2.0
Ac-RPLALWRSGGGC	MMP-7	SiO_2/APTES/AuNP	44.6 ± 4.5
Ac-RPLALWRSGGGC	MMP-7	bare Au	17.3 ± 2.1
Ac-RPLALWRSGGGC	MMP-2	SiO_2/pOEGMA/AuNP	1.8 ± 0.2

[a] These peptides are substrates for MMP-7. [b] MMP was spiked in human normal serum at a final concentration of 2 μg mL^{-1} (100 pmol mL^{-1}) and then the reaction mixture was added on respective surface followed by incubation for 60 min at 37 °C. [c] Thickness of the pOEGMA film was 27 nm. [d] Efficiencies were calculated from the relevant peak intensity according to the eq 1 in the Materials and Methods.

available in the SigmaPlot software program (ver 10.0, SYSTAT Software).

RESULT AND DISCUSSION

Scheme 1 depicts the synthetic procedure for generating *p*OEGMA films on a Si/SiO_2 substrate, as well as the procedure for assaying MMP activity using TOF-SIMS. The *p*OEGMA films were synthesized by SI-ATRP of OEGMA on a Si/SiO_2 substrate and then functionalized with amine groups by activating the terminal hydroxyl groups diverging from the methacrylate backbones with DSC and ethylenediamine. AuNPs were attached onto the NH_2-functionalized *p*OEGMA films (*p*OEGMA-NH_2) through electrostatic interactions, followed by chemisorption of the cysteine-terminated peptide substrate (Ac-RPLALWRSC or AC-RPLALWRSCGGGC). Our previous study revealed that AuNPs can enhance the emission of secondary ions of peptides, thus increasing the sensitivity of TOF-SIMS analyses.[26,27] Moreover, the AuNPs provide a larger surface area available for binding the cysteine-terminated peptide substrate. MMP activity was determined by measuring the change in the mass intensity of peptides on AuNPs using TF-SIMS before and after reaction by MMP-7.

To examine the effect of the nonbiofouling *p*OEGMA films on TOF-SIMS performance, we first attempted to track the stability of the mass signal intensity of the peptides after addition of the serum samples to AuNP-modified *p*OEGMA films. Following the addition of the serum samples to the film surface, the resulting surface was subjected to TF-SIMS analysis. We traced the characteristic ion peak of the cysteine-terminated peptide (i.e., Ac-RPLALWRSC) adsorbed onto the AuNPs. As a result, distinctive species of quasi-molecular secondary ions were clearly observed for $[M\text{H-SH-COOH}]^+$ and $[M\text{H-H-COOH}]^+$, instead of only $[M\text{H}]^+$. This might be caused by a loss of small functional groups during the process of secondary ion formation occurring at the surface of the AuNPs.[26] The surface without any *p*OEGMA film (i.e., SiO_2/APTES/AuNPs/peptide) resulted in a significantly decreased peak intensity (Figure 1a), and this seems to be due to the adsorption of serum proteins. On the other hand, the peak intensity arising from the surface with a *p*OEGMA film (i.e., SiO_2/*p*OEGMA-NH_2/AuNPs/peptide) displayed a small change (~10% decrease) (Figure 1b). To check the thickness effect of *p*OEGMA film, the different thicknesses of the films were varied by controlling the polymerization time. By ellipsometry, the *p*OEGMA films were revealed to have thicknesses ranging from 4 to 72 nm (Figure 2a). When the ratio of the peak intensities (I/I_0) at $[M\text{H-SH-COOH}]^+$ before and after serum treatment was investigated as a function of film thickness, it was found that *p*OEGMA films with a thickness of 27 nm displayed the greatest level of resistance against nonspecific adsorption of serum proteins (Figure 2b). SPR spectroscopy also revealed that the amount of serum proteins adsorbed on the *p*OEGMA films was much less than that on the *p*OEGMA-free surface (Figure 2c). However, in the case of *p*OEGMA films with thicknesses greater than 27 nm (i.e., 32 and 72 nm), the relative ratio of I/I_0 was considerably reduced. This result might be due mainly to the increased attachment of AuNPs, and subsequently, peptides as the functional groups (NH_2) increased. Considering that an increase in the thickness of the *p*OEGMA films gives rise to a higher surface density of amino groups due to the growth of divergent branches of the methacrylate backbone (Scheme 1), the use of *p*OEGMA films with thicknesses greater than 27 nm might lead to the attachment of excessive amounts of AuNPs, masking almost all of the exposed surface area of *p*OEGMA-NH_2. As a consequence, the decreased amount of exposure of nonbiofouling surfaces could cause an increase in the nonspecific adsorption of serum proteins. Consistent with this possibility, it was observed that before the addition of serum, the intensities of the peaks corresponding to the AuNPs and peptides (at $[Au_5]^+$ and $[M\text{H-SH-COOH}]^+$, respectively) increased with increasing thickness of *p*OEGMA-NH_2 (data not shown). In general, the ability to retain an acceptable level of fouling resistance is likely to be dependent on a delicate balance between the surface density of AuNPs and the thickness of *p*OEGMA-NH_2.

Given the effective blocking of nonspecific protein binding by the *p*OEGMA films, we proceeded to examine the effect of peptide length on the cleavage efficiency of MMP-7 on the film surfaces (Figure 3). Two peptide substrates with different lengths were compared (Ac-RPLALWRSC in Figure 3a and Ac-RPLALWRSGGGC in Figure 3b). MMP-7 specifically hydrolyzes the Ala−Lys bond,[35] and thus, the resulting mass signals represent the SI of the anchoring peptide (LWRSC or LWRSGGGC) after cleavage by MMP-7. As described by eq 1, the cleavage efficiency of MMP-7 was calculated from the ratio of the peak intensity of the cleaved peptide (I_c) to the peak intensity of the uncleaved original peptide (I_p) within a single spectrum. It is evident that the MMP-7 reaction resulted in a significant decrease in the original peak intensity of both peptide substrates, generating new positive $[M_c\text{H-SH-COOH}]^+$ ion signals at m/z 586 (bottom graph in Figure 3a) and 757 (middle graph in Figure 3b), which correspond to the peptide mass values (M_c) resulting from cleavage of the peptide substrates by MMP-7 for LWRSC and LWRSGGGC, respectively. However, in the case of peptides with no glycine linker, the cleavage efficiency (11.2%) was much lower than that (96.7%) calculated for peptides with a glycine linker. As a control, MMP-2 was also tested, but no peptide signals were observed (bottom graph in Figure 3b). It was expected that longer peptide substrates would have increased accessibility to the enzyme and, hence, undergo a more efficient protease reaction. However, it was found that for peptide substrates having a further longer length (e.g., Ac-

(35) Zhang, Y.; So, M. K.; Rao, J *Nano Lett.* **2006**, *6*, 1988–1992.

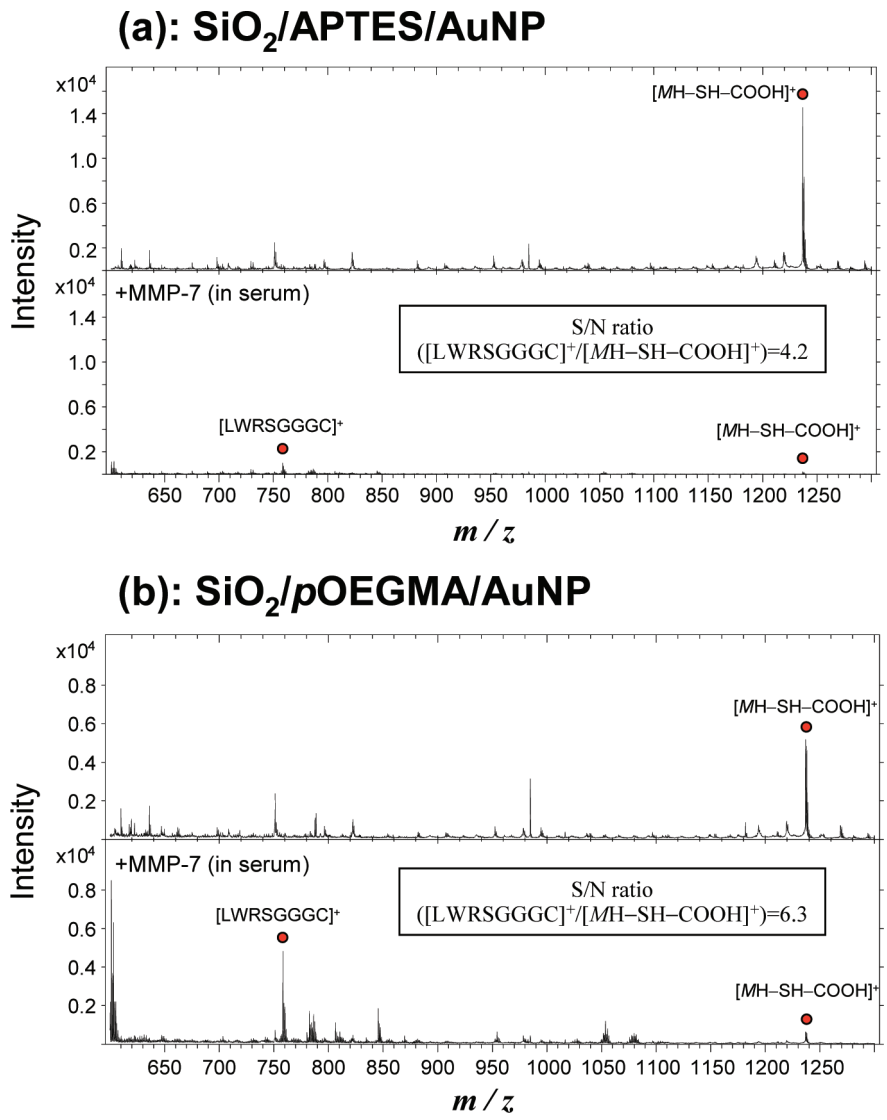

Figure 4. SIMS spectra for the activity of MMP-7 in human serum (a) on SiO_2/APTES/AuNP and (b) on SiO_2/*p*OEGMA/AuNP. MMP-7 was spiked in human normal serum at a final concentration of 2 μg mL^{-1}. The peaks of *m*/*z* 757 and 1237 represent the cleavage mass ion ([LWRSGGGC]$^+$) and the quasi-molecular ion ([*M*H-SH-COOH]$^+$) of Ac-RPLALWRSGGGC, respectively. The signal-to-noise ratio (peak intensity of *m*/*z* 757−1237) is presented in each surface.

RPLARS$(G)_7$C), protease activity was significantly lowered, and this seems to be due to limited signal enhancement in terms of the mass range (data not shown).

We additionally investigated the cleavage efficiency of MMP-7 spiked in serum. As shown in Table 1, the highest level of efficiency, approaching 93.6%, was observed for the Ac-RPLALWRSGGGC peptide substrate immobilized on the SiO_2/*p*OEGMA/AuNP surface. In contrast, the surfaces without *p*OEGMA (i.e., SiO_2/APTES/AuNP or bare Au) resulted in a significantly decreased level of MMP-7 activity, probably due to nonspecific adsorption of serum proteins. As shown in Figure 4, the signal intensity of the peptides was significantly reduced when MMP-7 was assayed in a serum environment. The signal-to-noise ratio (peak intensity of *m*/*z* 757−1237) of *p*OEGMA-immobilized surface (Figure 4a) was found to be higher than that of APTES-immobilized one (Figure 4b). These results clearly indicate that the *p*OEGMA film provides an effective surface platform for activity-based assays of protease in complex mixtures.

In further studies, we generated a calibration curve and determined the detection limit for assaying MMP-7 on the *p*OEGMA films. For these experiments, the assays were performed using a multiwell-type silicon coverslip as described in our previous study.[36] The calibration curve was obtained by plotting the observed cleavage efficiency as a function of the concentration of MMP-7 spiked in normal human serum (Figure 5). Normal human serum without any MMP-7 present, which confirmed by enzyme-linked immunosorbent assay (ELISA) (data not shown), was used as a control. There might be a variation in the actual amount of enzyme in assay solution due to supplemented additives in purchased enzyme solution, which affects detection limit of the assay. In this work, however, MMP-7 was dissolved in 10 mM HEPES buffer (pH7.4) only containing 150 mM NaCl and 5 mM $CaCl_2$. Under this condition, the effect of salts on the detection limit is likely to be marginal. Reaction mixtures containing different levels of MMP-7 were added to

(36) Kim, Y.-P.; Oh, Y.-H.; Kim, H.-S. *Biosens. Bioelectron.* **2008**, *23*, 980–986.

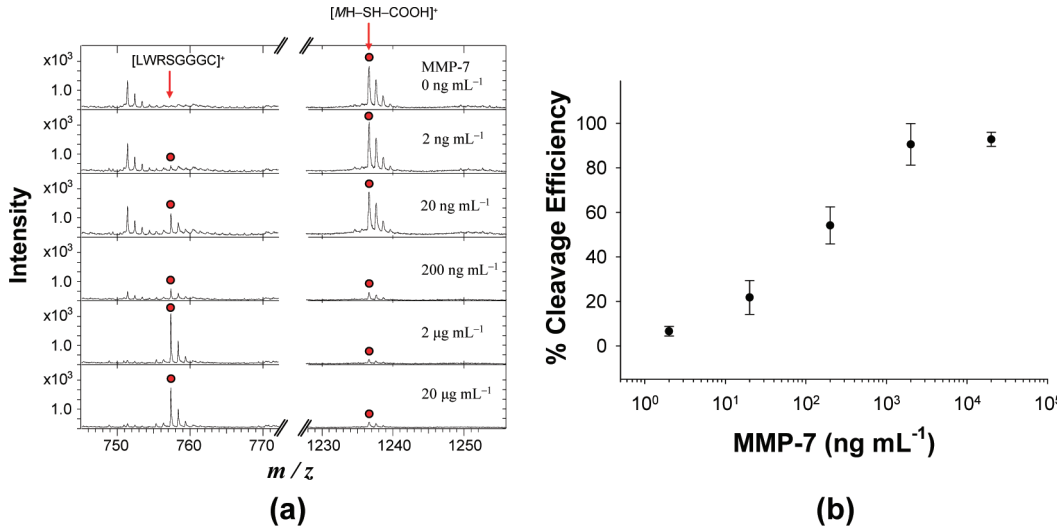

Figure 5. SIMS analysis of protease activity levels in human serum as a function of MMP-7 concentration. (a) SIMS spectra and (b) the corresponding standard curve. The peaks of m/z 757 and 1237 represent the cleavage mass ion ([LWRSGGGC]$^+$) and the quasi-molecular ion ([*M*H-SH-COOH]$^+$) of Ac-RPLALWRSGGGC, respectively. Varying concentrations of MMP-7 (ranging from 2 ng mL^{-1} to 20 μg mL^{-1}) were spiked in human normal serum, which was then added onto SiO_2/*p*OEGMA/AuNP/peptide surfaces. The MMP-7-free serum was used as a control. MMP-7 activity is expressed in terms of the cleavage efficiency for a given peptide substrate. Standard deviation values were obtained from the results of two independent experiments.

appropriate wells containing surfaces modified with SiO_2/*p*OEGMA/AuNP/peptide. As a result, the cleavage efficiency by MMP-7 was revealed to be linearly dependent on the logarithmic concentration of MMP-7, ranging from as low as 20 ng mL^{-1} to 2 μg mL^{-1}, which is a highly useful analytical range when considering the typical in vivo secretion levels within malignant tissues (>600 ng mL^{-1})[37] and cancer patient sera (>126 ng mL^{-1}).[38] Moreover, the detection sensitivity (20 ng mL^{-1}) of our assay system was found to be much higher than that recently reported for an analytical platform based on Förster resonance energy transfer, where detection sensitivity of collagenase was ~500 ng mL^{-1}.[39] These results provide strong supporting evidence that the *p*OEGMA films are a useful surface platform for carrying out highly sensitive assays of MMP activity in serum using TOF-SIMS.

In a final set of experiments to characterize the efficiency of the *p*OEGMA films in an inhibition assay, we also measured the activity of MMP-7 in the presence of varying concentrations of MMP-7 inhibitor (MMPI) (Figure 6). A significant decrease in MMP-7 activity was observed with increasing concentrations of minocycline, which is known to be a tetracycline MMP inhibitor with chelating properties in vivo.[40] The half-maximal inhibitory concentration (IC_{50}) of minocycline was estimated to be 450 nM. Based on this result, it seems that our assay platform can also be effectively used for inhibition assays of MMP with high sensitivity.

Unlike antibody-based immunoassay such as ELISA, the assay system presented in this work enables the direct assay of protease activity. This would be advantageous in the protease assay because the biologically active protease can be specifically assayed without interference by inactive or latent proforms of the enzyme (i.e., zymogen). More significantly, our label-free method on nonbiofouling surfaces allows a straightforward analysis of the enzyme activity even in a serum sample. Our approach would be suitable for studying modifications of substrates by many kinds of enzymes including kinases, phosphatase, acyltransferase, methylases, and other proteases in sera or cells.

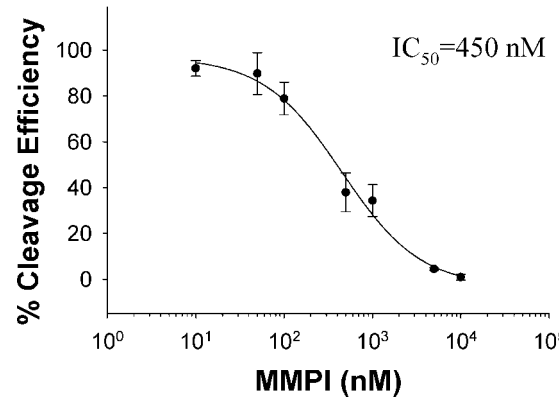

Figure 6. Inhibition assays of MMP-7 using SIMS. Varying concentrations of MMP inhibitor (MMPI, minocycline) were premixed in a reaction solution containing MMP-7 (2 μg mL^{-1}), which was then added onto SiO_2/*p*OEGMA/AuNP/peptide surfaces. Standard deviation values were obtained from the results of two independent experiments.

CONCLUSION

We have demonstrated an effective activity-based assay of MMP-7 on peptide-conjugated AuNPs with nonbiofouling *p*OEGMA films using TOF-SIMS. Despite the fact that proteases play a crucial role in normal cellular function, sensitive assays of these enzymes have been severely hampered by the presence of interfering proteins in human serum. However, by employing

(37) Watelet, J. B.; Bachert, C.; Claeys, C.; Van Cauwenberge, P. *Allergy* **2004**, *59*, 54–60.
(38) Maurel, J.; Nadal, C.; Garcia-Albeniz, X.; Gallego, R.; Carcereny, E.; Almendro, V.; Marmol, M.; Gallardo, E.; Maria Auge, J.; Longaron, R.; Martinez-Fernandez, A.; Molina, R.; Castells, A.; Gascon, P. *Int. J. Cancer* **2007**, *121*, 1066–1071.
(39) Shi, L.; De Paoli, V.; Rosenzweig, N.; Rosenzweig, Z. *J. Am. Chem. Soc.* **2006**, *128*, 10378–10379.
(40) Paemen, L.; Martens, E.; Norga, K.; Masure, S.; Roets, E.; Hoogmartens, J.; Opdenakker, G. *Biochem. Pharmacol.* **1996**, *52*, 105–111.

*p*OEGMA films as a nonbiofouling surface platform in TOF-SIMS, we showed that high analytical sensitivity for clinically relevant concentrations of MMP-7 can indeed be attained even in human serum. We anticipate that our straightforward label-free approach employing TOF-SIMS on nonbiofouling surfaces will offer an effective format for activity-based assays of proteases and their inhibition in a sensitive, high-throughput manner.

ACKNOWLEDGMENT

This work was supported by the Next-Generation New-Technology Development Program for MKE, the Nano Science & Technology Program (M10503000868-07M0300-86810), the Brain Korea 21 Program, Biosignal Analysis Technology Innovation Program (M1064501000002-06N4501-00210), and the Nano/Bio Science & Technology Program (M10536090002-07N3609-00210) of MEST, the Korea Health 21C R&D Project (0405-MN01-0604-0007) of MIHWAF, and the Korea Science and Engineering Foundation Grant (R01-2005-000-10355-0). The ellipsometer were purchased with a research fund from the Center for Molecular Design and Synthesis. We thank Dr. Kyung-Bok Lee at KBSI for the expert technical assistance.

Received for review February 12, 2008. Accepted April 22, 2008.

AC800299D